Polyhedron 99 (2015) 26–33

Contents lists available at ScienceDirect

Polyhedron

journal homepage: www.elsevier.com/locate/poly

Two novel organic–inorganic hybrid compounds with straight and zigzag chain alignments of Cu(II) centers: Synthesis, crystal structure, spectroscopy, thermal analysis and magnetism

Justin Nenwa [a,c,*], Edith D. Djomo [a], Emmanuel N. Nfor [b], Patrick L. Djonwouo [a], Mohammed Mbarki [c], Boniface P.T. Fokwa [c,*]

[a] Department of Inorganic Chemistry, University of Yaounde 1, P.O. Box 812, Yaounde, Cameroon
[b] Department of Chemistry, University of Buea, P.O. Box 63, Buea, Cameroon
[c] Institute for Inorganic Chemistry, RWTH Aachen University, D-52056 Aachen, Germany

ARTICLE INFO

Article history:
Received 5 May 2015
Accepted 11 June 2015
Available online 25 June 2015

Keywords:
Hybrid salts
Oxalate copper(II) complexes
Stacking pattern
Magnetic properties
Crystal structures

ABSTRACT

Two hybrid salts, *viz.* bis(guanidinium) bis(oxalato)cuprate(II) (**1**) and bis(2-aminopyridinium) bis(oxalato)cuprate(II) trihydrate (**2**) have been synthesized and characterized by elemental and thermal analyses, IR spectroscopy, single-crystal X-ray diffraction and SQUID magnetometry. Compounds **1** and **2** crystallize in the monoclinic $P2_1/c$ and triclinic $P\bar{1}$ space groups, respectively. In both structures, the four-coordinated Cu(II) ion in $[Cu(C_2O_4)_2]^{2-}$ unit weakly interacts with two axial O-atoms of neighboring units to build a prolate CuO_6 octahedron, with regular axial Cu–O bonds of 2.825 Å in **1**, whereas in **2** two different Cu–O bonds (2.814 Å and 2.701 Å) are found. In **1**, stacking of $[Cu(C_2O_4)_2]^{2-}$ units across internal symmetry-related O-atoms results in equidistantly spaced monomers, thus forming straight Cu(II) chains with regular spacing of Cu···Cu = 3.582 Å. By contrast, in **2**, stacking of the $[Cu(C_2O_4)_2]^{2-}$ entities occurs via *external* symmetry-related O-atoms, yielding zigzag Cu(II) chains with shorter *intra*-dimer spacing of $[Cu\cdots Cu]_{intra}$ = 3.430 Å and longer *inter*-dimer spacing of $[Cu\cdots Cu]_{inter}$ = 4.961 Å. The anhydrated compound **1** is stable up to 250 °C, whereas the hydrated compound **2** shows a significant weight loss of solvent water molecules at about 70 °C, followed by the decomposition of the network. The magnetic measurements in the 2–300 K temperature range revealed weak antiferromagnetic coupling in the two hybrid salts.

1. Introduction

Recently, organic–inorganic hybrid salts have been introduced as an attractive area of study within the field of crystal engineering [1–3]. The flourishing diversity of structures and dimensionalities observed in these multifunctional materials has aroused a remarkable research interest [4,5]. As a result of structural integration of organic cations and inorganic counterparts, molecular electronic and spintronic [6], peculiar magnetic [7,8], optical [9,10], metallic conductivity [11] and catalytic [12] properties have arisen in this class of chemical hybrid systems. Moreover, these materials may be used as model compounds for ferroelectric and ferroelastic applications [13,14]. Self assembly processes of such materials in solid state are due to the variety of interactions which include hydrogen bonding network between organic and inorganic components, ionic interactions, π–π and/or van der Waals interactions [15–17].

Over the past years, many salts of organic cations combined to the well-known bis(oxalato)cuprate(II) anion have been intensely studied among other reasons for their fascinating network topologies as well as for gaining a better understanding of the correlations between structural and physical properties [18–20]. In these salts, the steric parameters of the organic cations, the nature of the additional ligand or solvent molecule, and the medium of the synthesis are thought to be the notable factors to affect the obtained frameworks which, indeed, are still difficult to be predicted and controlled. For example, pyridinium cations combined to bis(oxalato)cuprate(II) anions lead to the formation of hydrogen-bonded copper(II) chain structures [19]. Benzylammonium copper(II) oxalate salt results in layers of $[Cu(C_2O_4)_2]^{2-}$ ions connected by long axial Cu–O bonds [20].

* Corresponding authors at: Institute for Inorganic Chemistry, RWTH Aachen University, D-52056 Aachen, Germany.
E-mail addresses: jnenwa@yahoo.fr (J. Nenwa), boniface.fokwa@ac.rwth-aachen.de (B.P.T. Fokwa).

http://dx.doi.org/10.1016/j.poly.2015.06.023
0277-5387/

With propylenediammonium cations, stacks of bis(oxalato)cuprate(II) anions are obtained [20]. This flexibility of the structural topology in (organic cation)-oxalatocuprate(II) compounds bears testimony to the renewed interest in their coordination chemistry.

In the present paper, we report on the structural characterization of two novel copper(II) hybrid salts bis(guanidinium) bis(oxalato)cuprate(II), $(CN_3H_6)_2[Cu(C_2O_4)_2]$ (**1**), and bis(2-aminopyridinium) bis(oxalato)cuprate(II) trihydrate, $(C_5H_7N_2)_2[Cu(C_2O_4)_2]\cdot 3H_2O$ (**2**), the structures of which the common anionic bis(oxalato)cuprate(II) entities exhibit different stacking patterns. Low temperature magnetic studies reveal weak antiferromagnetic behavior in both compounds.

2. Experimental

2.1. Materials and physical measurements

Oxalic acid dihydrate, chromium(III) chloride hexahydrate, 2-aminopyridine and copper(II) oxalate hemihydrate were purchased from Riedel de Haën. The guanidinium carbonate salt was obtained from Aldrich and the starting compound, $K_2[Cu(C_2O_4)_2(H_2O)_2]$, was prepared following the literature procedure [21]. All the chemicals were used without further purification and the chemical reactions were carried out in distilled water as the solvent. Elemental analysis (C, H, N) was performed on a Vario EL (Heraeus) CHNS analyzer. The infrared spectra were recorded on a Perkin–Elmer (System 2000) FT-IR spectrometer with a pressed KBr pellet in the scan range 4000–400 cm^{-1} and the UV–Vis spectra on a Perkin–Elmer Lambda 900 spectrophotometer, in water solution, in the range 200–800 nm ($c = 5.571 \times 10^{-5}$ mol/L). Thermal analyses (TGA and TDA) were performed with a Mettler Toledo TGA/SDTA 851 thermal analyzer. The powdered sample (*ca.* 15 mg) was heated from 25 to 600 °C with a rate of 10 °C/min in dry nitrogen gas flowing at 60 mL/min. Magnetic susceptibility data for the polycrystalline complexes **1** and **2** were recorded using a Quantum Design MPMS-5XL SQUID magnetometer in the temperature range 2–300 K at an applied magnetic field of 0.1 T. The diamagnetic corrections of the constituent atoms were estimated from Pascal's constants [22]. The effective magnetic moment was calculated as $\mu e_{ff}(T) = [(3k/N_A\mu_B^2)\chi T]^{1/2} \approx (8\chi T)^{1/2}$.

2.2. Syntheses

2.2.1. Synthesis of $(CN_3H_6)_2[Cu(C_2O_4)_2]$ (**1**)

An aqueous solution (20 mL) of guanidinium carbonate (180 mg, 1 mmol) was added dropwise to a blue solution of $K_2[Cu(C_2O_4)_2(H_2O)_2]$ (350 mg, 1 mmol) in 30 mL of warm water. The mixture was stirred at 50 °C for 1 h. After cooling to room temperature, the resulting solution was filtered, and the filtrate was allowed to stand undisturbed at room temperature for about one week. Blue-greenish single crystals were isolated by filtration and dried in air. Yield: 80%. *Anal.* Calc. for $C_6H_{12}CuN_6O_8$ (359.76): C, 20.03; H, 3.36, N, 23.36. Found: C, 20.02; H, 3.33, N, 23.56%. IR (cm^{-1}): 3470m, 1710m, 1660s, 1610m, 1410m, 1280m, 800w, 553w.

2.2.2. Synthesis of $(C_5H_7N_2)_2[Cu(C_2O_4)_2]\cdot 3H_2O$ (**2**)

$H_2C_2O_4\cdot 2H_2O$ (126 mg, 1 mmol) and 2-aminopyridine (188 mg, 2 mmol) were dissolved in warm water (30 mL), giving a yellowish solution. $CuC_2O_4\cdot 1/2H_2O$ (72 mg, 0.5 mmol) was added in successive small portions to the above solution and the mixture stirred at 60 °C for 1 h and then cooled to room temperature under ambient conditions. The resulting green solution was filtered and left to stand in the hood at room temperature. After two days, elongated crystals were isolated by filtration and dried in air. Yield: 72%. *Anal.* Calc. for $C_{14}H_{14}CuN_4O_8$ (429.88) which is the non-hydrated form of $C_{14}H_{20}CuN_4O_{11}$ (483.88): C, 39.08; H, 3.26, N, 13.03. Found: C, 39.16; H, 3.24, N, 13.05%. IR (cm^{-1}): 3310m, 3150m, 1710s, 1670s, 1630s, 1480w, 1400m, 1270m, 1000w, 802w, 763w, 552w.

2.3. X-ray crystallography

Appropriate single crystals of **1** and **2** were mounted in random orientation on a glass fiber. Intensity data were collected at 293 K on a Bruker APEX CCD area-dectector diffractometer with graphite-monochromatized Mo Kα radiation ($\lambda = 0.71073$ Å). The X-ray intensities were corrected for absorption using a semi-empirical procedure [23]. The structures were solved by direct methods with SHELXS-97 [24] and refined by full-matrix least squares method based on F^2 with SHELXL-97 [24]. All non-hydrogen atoms were refined anisotropically. The positions of hydrogen atoms were added in idealized geometrical positions for the organic cations. The positions of hydrogen atoms from the water molecules were assigned from the electronic density map generated by Fourier difference and they were refined freely. The ORTEP-3 program [25] was used within the winGX software package [26] to deal with the processed crystallographic data and artwork representations. Crystal data and structure refinement parameters for **1** and **2** are given in Table 1, selected bond lengths and bond angles in Table 2.

Table 1
Crystal data and structure refinement for **1** and **2**.

Compound	**1**	**2**
Empirical formula	$C_6H_{12}CuN_6O_8$	$C_{14}H_{20}CuN_4O_{11}$
Formula weight	359.76	483.88
T (K)	293(2)	293(2)
λ (Å)	0.71073	0.71073
Crystal system	monoclinic	triclinic
Space group	$P2_1/c$	$P\bar{1}$
Unit cell parameters		
a (Å)	3.5821(4)	7.7104(17)
b (Å)	15.7044(17)	9.159(2)
c (Å)	11.2936(12)	14.853(3)
α (°)	90	72.902(3)
β (°)	96.968(2)	88.896(3)
γ (°)	90	77.962(3)
V (Å^3)	630.63(12)	979.5(4)
Z	2	2
D_{calc} (g/cm^3)	1.895	1.641
μ (mm^{-1})	1.787	1.182
$F(000)$	366	498
Crystal size (mm)	0.18 x 0.03 x 0.01	0.18 x 0.03 x 0.01
θ range for data collection (°)	5.19 – 36.15	4.68 – 33.02
Index ranges	$-5 < h < 5$, $-25 < k < 23$, $-18 < l < 12$	$-11 < h < 9$, $-12 < k < 14$, $-22 < l < 22$
Total reflections	6805	9477
Unique reflections (R_{int})	2765 (0.0257)	6919 (0.0419)
Max. and min. transmission	0.988 and 0.813	0.988 and 0.813
Refinement method	full-matrix least squares on F^2	full-matrix least squares on F^2
Data/restraints/parameters	1987/0/121	3456/9/348
Goodness-of-fit (GOF) on F^2	1.057	0.990
R factor [$I > 2\sigma(I)$]	$R_1 = 0.0397$, $wR_2 = 0.0944$	$R_1 = 0.0686$, $wR_2 = 0.1201$
R factor (all data)	$R_1 = 0.0634$, $wR_2 = 0.1122$	$R_1 = 0.1515$, $wR_2 = 0.1569$
Max and min residual electron density (e/Å^3)	0.521 and −0.365	2.679 and −1.947

Table 2
Selected bond lengths (Å) and bond angles (°) within the coordination spheres around the metal centers in **1** and **2**.

Compound (**1**)			
Cu1–O1	1.9218(14)	O1–Cu1–O1^{i}	180.00(5)
Cu1–O1^{i}	1.9218(14)	O1–Cu1–O2^{i}	94.41(6)
Cu1–O2^{i}	1.9350(14)	O1^{i}–Cu1–O2^{i}	85.59(6)
Cu1–O2	1.9350(14)	O1–Cu1–O2	85.59(6)
		O1^{i}–Cu1–O2	94.41(6)
		O2^{i}–Cu1–O2	180.00(5)
Compound (**2**)			
Cu1–O5	1.909(2)	O5–Cu1–O2	174.69(12)
Cu1–O2	1.920(2)	O5–Cu1–O1	94.6(1)
Cu1–O1	1.933(3)	O2–Cu1–O1	85.37(11)
Cu1–O6	1.945(2)	O5–Cu1–O6	85.27(10)
		O2–Cu1–O6	94.94(10)
		O1–Cu1–O6	177.97(11)

Symmetry transformations used to generate equivalent atoms for (**1**): (i) $-x$, $1-y$, $1-z$.

3. Results and discussion

3.1. Crystal structure of *1*

Compound **1** crystallizes in the monoclinic $P2_1/c$ space group. Its molecular structure and crystallographic atom numbering are illustrated in Fig. 1(left). The crystal structure of **1** consists of one dianionic copper(II) oxalate complex, $[Cu(C_2O_4)_2]^{2-}$, and two guanidinium cations, $(CN_3H_6)^+$. The copper(II) ion is at the center of symmetry and it coordinates to four oxygen atoms of two oxalato(2-) ligands (average Cu–O length: 1.9284 Å) in the equatorial plane, and axially, weakly bonds to the coordinated oxygen atoms of the oxalate from the neighboring complexes (regular axial Cu–O2 contacts: 2.825 Å), giving rise to a distorted elongated octahedral geometry. The basal CuO_4 plane is planar due to symmetry restriction, and the O–Cu–O bite angle within the plane is 85.59(6)°, a value which is similar to those found in previously reported metal complexes [19,27,28]. As shown in Fig. 2(left), the stacking of the $[Cu(C_2O_4)_2]^{2-}$ entities in **1** occurs across symmetry-related O2 atoms, resulting in equidistantly spaced monomers and forming straight Cu(II) chains with regular spacing of Cu···Cu = 3.582 Å parallel to [1 0 0], in agreement with the value observed in the most closely related salt $(C_5H_6N)_2[Cu(C_2O_4)_2]\cdot H_2C_2O_4$ (Cu···Cu: 3.697(7) Å [19]. It deserves to be noted that the stacking of $[Cu(C_2O_4)_2]^{2-}$ units in $Na_2[Cu(C_2O_4)_2]\cdot 2H_2O$ [29] is similar to that of compound **1**, with axial Cu–O distances equal to 2.803(2) Å and Cu···Cu separations of 3.576(2) Å. In contrast, the structure of compound **1** is markedly different from that of the propylenediammonium [20], potassium and ammonium [30] derivatives even though the stacking of the $[Cu(C_2O_4)_2]^{2-}$ units in all these compounds leads to straight chain alignment of copper(II) centers. Indeed, in the propylenediammonium bis(oxalate)cuprate(II) salt, $(C_3H_6N_2H_6)[Cu(C_2O_4)_2]$, the stacking of the anions is made through a bridging involving a non-coordinated oxygen atom of oxalate, with long axial Cu–O contacts of 2.883(3) Å. Thus, the repeat Cu···Cu spacing along the chain (4.920 Å) is appreciably larger than that (3.582 Å) of compound **1**. On the other hand, the crystal structures of the isostructural salts $K_2[Cu(C_2O_4)_2]\cdot 2H_2O$ [30] and $(NH_4)_2[Cu(C_2O_4)_2]\cdot 2H_2O$ [30]

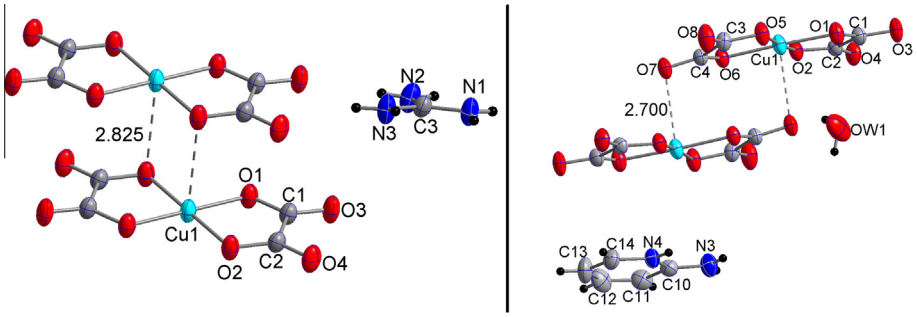

Fig. 1. ORTEP drawing of the ionic constituents of **1** (*left*) and **2** (*right*) with the atom numbering scheme. Displacement ellipsoids are drawn at the 50% probability level.

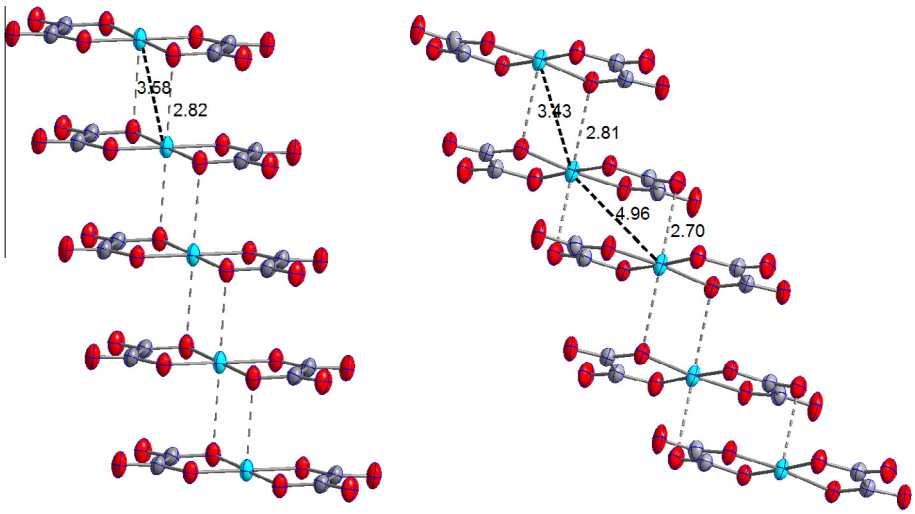

Fig. 2. Straight (*left*) and zigzag (*right*) chain alignments of Cu(II) centers in compounds **1** and **2**, respectively.

are not made of columnar stacks of units $[Cu(C_2O_4)_2]^{2-}$ but they contain units $[Cu(C_2O_4)(H_2O)_2]^{2-}$ and units $[Cu(C_2O_4)_2]^{2-}$ connected through terminal oxygen atoms of oxalate, with Cu···Cu separations of more than 5 Å [31]. As consequence of these different behaviors of the anions stacking the resulted magnetic Cu···Cu interactions in compound **1** will be similar to those found in $Na_2[Cu(C_2O_4)_2]\cdot 2H_2O$ (see below). The bond distances and angles in the guanidinium cation show no significant difference from those obtained in reported salts involving the same organic group [32,33]. These organic cations are packed along the *a* axis and contribute to stabilize the crystal packing through N–H···O hydrogen bonds (Fig. 3). The distances and angles of the hydrogen bonds are listed in Table 3. In addition, intrachain π···π interactions between oxalate groups further enhance the cohesion of this structure.

3.2. Crystal structure of **2**

Compound **2** crystallizes in the triclinic $P\bar{1}$ space group. As shown in Fig. 1(right), the basic structure units of **2** consist of $[Cu(C_2O_4)_2]^{2-}$ anions, 2-aminopyridinium cations, $(C_5H_7N_2)^+$, and water molecules. The copper atom has a strongly distorted octahedral geometry with four O atoms (O1, O2, O3 and O4) from one bis(oxalato)cuprate(II) on the equatorial plane and two O atoms on the axial position. The equatorial Cu–O bond lengths diverge just slightly from one another as they range from 1.909(2) to 1.945(2) Å, while much longer axial Cu–O bonds (2.701 Å and 2.814 Å) are found. The stacking of the $Cu(C_2O_4)_2]^{2-}$ anions is distinctly different in compounds **1** and **2**. In this latter salt, one $Cu(C_2O_4)_2]^{2-}$ unit is linked, via the 2.701 distance, to the second by a terminal oxalate oxygen atom (O7) which appears at the axial position of the second copper site, thus forming a centrosymmetric dimer. As illustrated in Fig. 2(right), the stacking of these dimers occurs across *external* symmetry-related O8 atoms, via the 2.814 distance, yielding zigzag Cu(II) chains with shorter *intra*dimer spacing of $[Cu\cdots Cu]_{intra}$ = 3.430 Å and longer *inter*dimer spacing of $[Cu\cdots Cu]_{inter}$ = 4.961 Å parallel to [100]. The value found for the *inter*dimer contact is in agreement with that reported in the dimeric copper(II) complex of oxalate and oxamide dioxime ligands (2.803 Å) [27]. In contrast, the *inter*dimer spacing Cu···Cu is significantly longer, compared to the data observed earlier [19,27,28]. The packing diagram of **2** is depicted in Fig. 4, highlighting water-filled (top) and empty (bottom) nanochannels oriented parallel to [100]. There are six water molecules of crystallization per unit cell within the channel. A section of the unit cell of **2** (Fig. 5) highlights the intra- and intermolecular hydrogen bonds (dashed lines, *left*) and a hexamer of H-bonded water molecules (*right*). These hexameric water molecules per unit cell are linked

Table 3
Hydrogen bond lengths (Å) and angles (°) for (**1**) and (**2**).

D–H···A	*d*(D–H)	*d*(H···A)	*d*(D···A)	<(DHA)
$(CN_3H_6)_2[Cu(C_2O_4)_2]$ (**1**)				
N1—H1A—O3^{i}	0.83(3)	2.19(3)	2.995(3)	165.(3)
N1—H1B—O4^{ii}	0.80(3)	2.28(3)	3.015(3)	154.(3)
N3—H2A—O4^{iii}	0.84(4)	2.24(3)	2.946(3)	142.(3)
N3—H2A—O3^{iii}	0.84(4)	2.37(4)	3.085(3)	144.(3)
N3—H2B—O4^{ii}	0.84(3)	2.35(3)	3.041(3)	139.(3)
N2—H3B—O3^{iii}	0.79(3)	2.29(4)	3.014(3)	151.(3)
N2—H3A—O1^{i}	0.82(3)	2.12(3)	2.925(3)	166.(3)
$(C_5H_7N_2)_2[Cu(C_2O_4)_2]\cdot 3H_2O$ (**2**)				
N1—H1A—O3^{i}	0.83(5)	2.21(5)	3.032(5)	171.(4)
N1—H1B—O8^{ii}	0.72(4)	2.24(4)	2.953(5)	170.(5)
N3—H3A—O4^{iii}	0.84(4)	2.12(5)	2.958(5)	172.(4)
N3—H3B—O7^{iv}	0.73(4)	2.32(5)	3.026(5)	165.(5)
N4—H4—O2^{iii}	0.83(4)	1.99(4)	2.804(4)	166.(4)
OW1—H1WB—O3^{i}	0.799(10)	2.19(3)	2.944(5)	157.(6)
OW2—H2WA—OW3	0.807(10)	2.003(14)	2.807(7)	175.(7)
OW2—H2WB—O3^{i}	0.801(10)	2.19(4)	2.883(4)	145.(6)
OW3—H3WB—OW1^{v}	0.799(10)	2.072(15)	2.865(6)	171.(5)
OW3—H3WA—OW2^{vi}	0.80(1)	2.054(15)	2.839(7)	167.(5)

Symmetry transformations used to generate equivalent atoms (D, donor; A, acceptor) : (i) *x*, 1.5 − *y*, −0.5 + *z*; (ii) 1 − *x*, 1 − *y*, 1 − *z*; (iii) −1 + *x*, *y*, −1 + *z* for (**1**) and (i) −1 + *x*, *y*, *z*; (ii) *x*, −1 + *y*, *z*; (iii) 1 − *x*, 1 − *y*, −*z*; (iv) −*x*, 2 − *y*, −*z*; (v) 1 − *x*, 1 − *y*, 1 − *z*; (vi) −*x*, 1−*y*, 1 − *z* for (**2**).

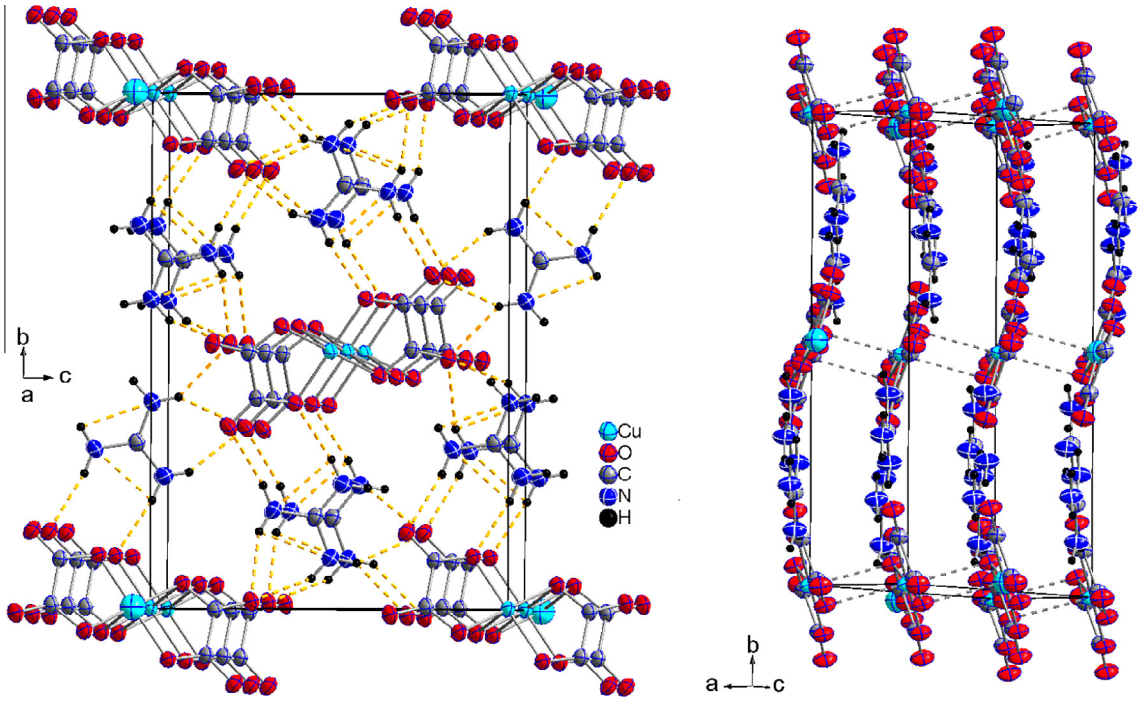

Fig. 3. Crystal packings of **1** highlighting the intra- and intermolecular hydrogen bonds (dashed lines, *left*) and wave-like planes (*right*). All hydrogen bonds are found within the planes.

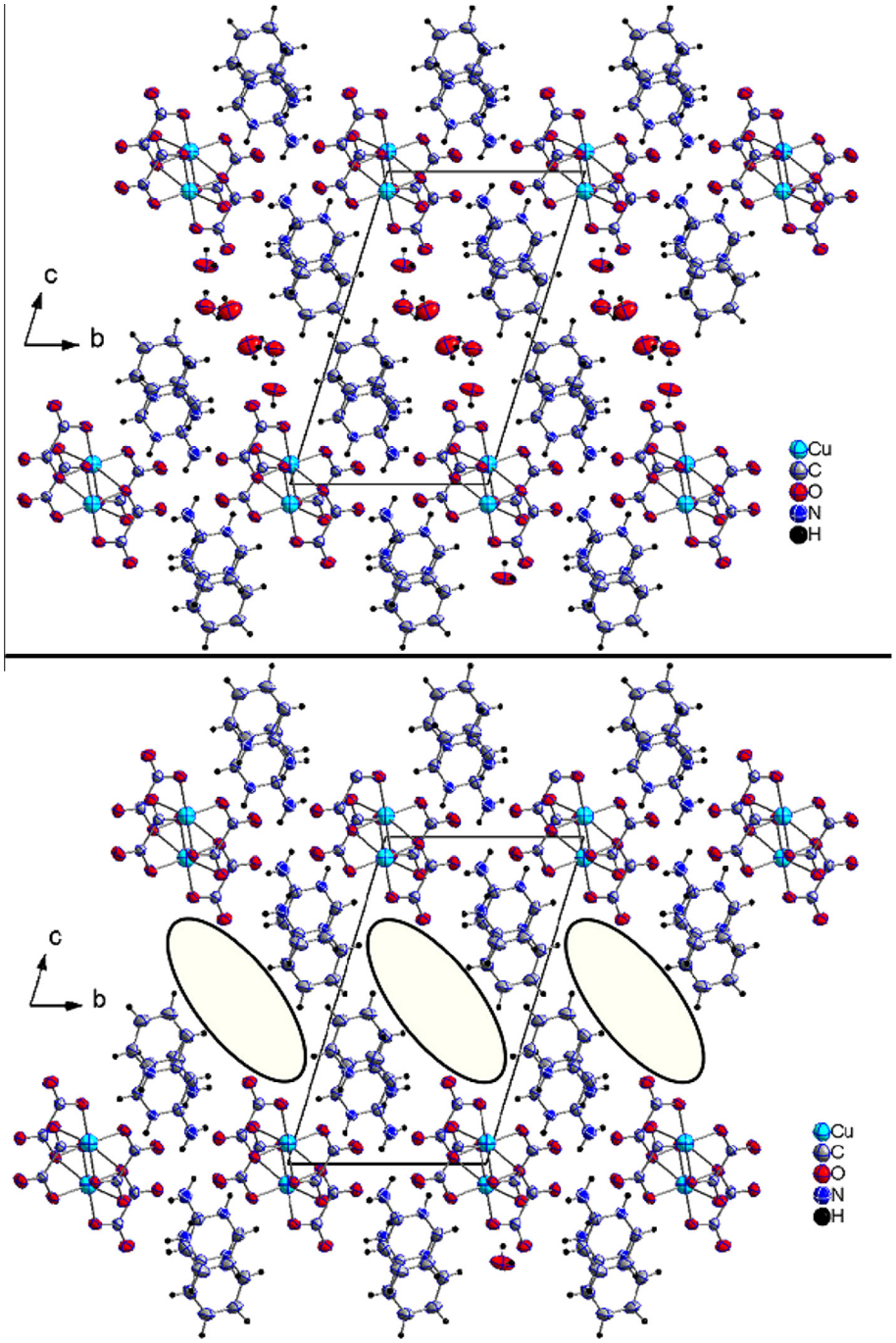

Fig. 4. Crystal packings of **2** highlighting water-filled (top) and empty (bottom) nanochannels.

in the form of a symmetrically twice branched slightly distorted rhombus. Compound **2** is another example of a closely related solid material encapsulating water cluster patterns that fit into the Infantes–Motherwell classification [34]. Two main categories of weak H-bonds are effective in this structure (Table 3). N–H···O bridges link either the amino N–H group to the free oxalato O atom or the protonated N atom to the coordinated oxalate O atom, with N···O separation ranging from 2.804(4) to 3.032(5) Å. Finally, the O–H···O bridges link water molecules not only amongst themselves but also to the free oxalato O atoms, with O···O separation ranging from 2.807(7) to 2.944(5) Å. Elemental analysis findings indicate that aged crystals of compound **2** are prone to lose progressively the three solvate waters of crystallization per formula unit. The pronounced tendency of this compound to release its lattice water molecules might be related to the weakness of these H-bonds interconnecting the ionic partners amongst themselves into the three dimensional host lattice.

3.3. Thermal analyses of *1* and *2*

Thermogravimetric analyses of compounds **1** and **2** were undertaken in the temperature range of 25–600 °C under flowing N_2 atmosphere at a heating rate of 10 °Cmn^{-1}, leading to the simultaneous TGA/DTA profiles. Compound **1** is thermally stable up to ca 250 °C followed by its decomposition which takes place in two major endothermic stages. Between 250 and 310 °C, the first

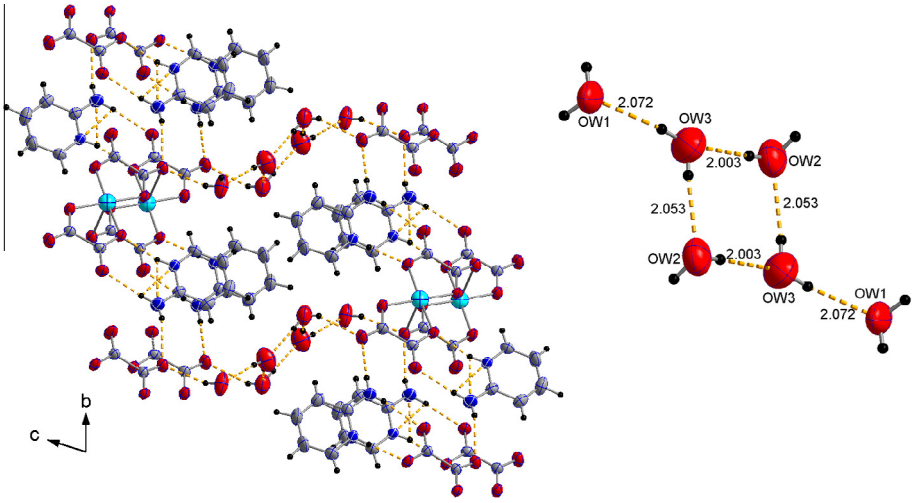

Fig. 5. Section of the unit cell of **2** highlighting the intra- and intermolecular hydrogen bonds (dashed lines, *left*) and a hexamer of H-bonded water molecules (*right*).

weight loss of 43.6% (calc. 44.5%) is due to the release of the combined mass of ($2N_2$+$2H_2$+$2CO_2$+CO) from a partial degradation of organic moieties. Between 310 and 435 °C, the second weight loss of 13.86% (calc. 13.34%) occurs, which corresponds to the decomposition of half of the by-product, $(NH_4)_2CO_3$. On further heating, the thermal degradation is completed and the final residue is proved to be CuO.

Contrary to the case of **1**, compound **2** is thermally stable up to only ca. 70 °C, and it undergoes three-step endothermic processes thereafter. In the temperature range of 70–82 °C, compound **2** suffers a first weight loss of 10.71% (calc. 11.16%) corresponding to the release of $3H_2O$. A second and significant weight loss of 66.55% (calc. 66.83%) occurs between 220 and 260 °C, corresponding to the decomposition of the framework and formation of $CuC_2O_4{\cdot}1/2H_2O$. From 260 to 315 °C, a third weight loss of 7.98% (calc. 7.65%) is consistent with the release of CO+$1/2H_2O$, the final residue being $CuCO_3$.

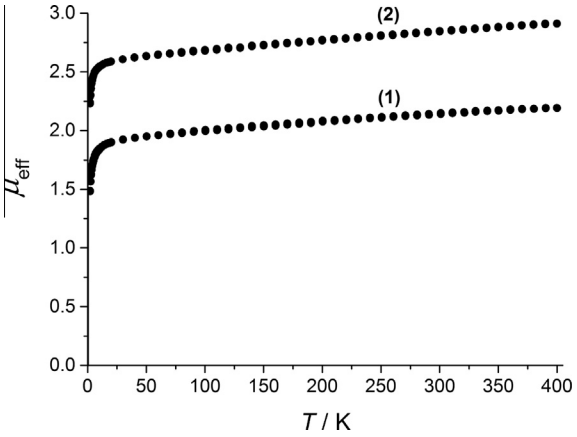

Fig. 6. Temperature-dependent magnetic behavior of **1** (bottom) and **2** (top).

3.4. Magnetic behaviors of *1* and *2*

Variable temperature magnetic susceptibility measurements (2.0–300 K) were carried out on powdered samples of the complexes taken from the same uniform batches used for structural determinations. The temperature dependences of the effective magnetic moments (μ_{eff}) for compounds **1** and **2** are plotted in Fig. 6. The shapes of μ_{eff} versus T curves are very similar, but the absolute values are different.

At 300 K, the effective magnetic moment of compound **1** is 1.90 μ_B, a value which is a little higher than that expected (1.73 μ_B) for the spin-only value for a mononuclear Cu(II) complex. In the lower temperature range, μ_{eff} rapidly decreases to reach the value of 1.5 μ_B at 2.0 K (Fig. 6), revealing therefore the occurrence of weak antiferromagnetic interactions between the copper(II) ions [35–38]. A behavior already found in $Na_2[Cu(C_2O_4)_2]{\cdot}2H_2O$ [29], whose crystal structure also contains the same stacking as in **1**.

At 300 K, the effective magnetic moment μ_{eff} of compound **2** (Fig. 6) is 2.75 μ_B. This μ_{eff} gradually decreases upon lowering the temperature from 2.75 μ_B at 300 K to 2.62 μ_B at around 40 K, and then abruptly decreases to reach the value of 2.30 μ_B at 2 K. This temperature-dependent behavior is similar to that of compound **1** and it also suggests weak antiferromagnetic interactions between the magnetic centers. It merits to be pointed out that μ_{eff} of 2.75 μ_B at 300 K for compound **2** is just slightly smaller than twice the expected spin-only value (1.73 μ_B) of a mononuclear Cu(II) complex. In fact, this value is much closer to those found in the dinuclear Cu(II) complexes $[Cu_2(C_2O_4)_2(H_2oxado)_2(H_2O)_2]$ (2.62 μ_B per dimer) [27], $[Cu_2(dpyam)_4(\mu\text{-}C_2O_4)](ClO_4)_2{\cdot}3H_2O$ (2.62 μ_B per dimer) [39], and $[Cu_2(dpyam)_4(\mu\text{-}C_2O_4)](BF_4)_2{\cdot}3H_2O$ (2.64 μ_B per dimer) [39]. This confirms our description of the crystal structure of compound **2** above, as a chain of dimers.

It has been shown that magnetic exchange interactions for oxalato-bridged Cu(II) complexes are strongly influenced by the geometry around the Cu(II) ions, the orientation of the magnetic orbitals in respect to the oxalate plane and the bridging mode of the oxalate group as well [40,41]. Structural data and magnetic properties for some selected oxalato-bridged Cu(II) complexes are summarized in Table 4. The weak intrachain antiferromagnetic coupling observed in compounds **1** and **2** can be attributed to a δ type interaction between the magnetic orbitals of $[Cu(C_2O_4)_2]^{2-}$ units [19,29–31]. These magnetic orbitals are built from the $dx^2 - y^2$ Cu(II) orbitals pointing toward oxygen atoms O of oxalate groups bound to Cu(II) ions. The unpaired electrons in the $dx^2 - y^2$ orbitals on adjacent copper ions interact with the σ framework on the oxalate ion in nearly orthogonal manner. Thus, the $[Cu(C_2O_4)_2]^{2-}$ planes in the double oxygen-bridged Cu(II) units are almost oriented parallel to each other. Such a molecular configuration is more favorable for the overlapping of magnetic orbitals of neighboring metal ions, leading to antiferromagnetic coupling

Table 4
Structural data and magnetic properties for 9 selected oxalato-bridged Cu(II) complexes.

Compound[a]	Cu(II) coord.[b]	Stacking mode[c]	Cu–O_{ax} (Å)	Cu–Cu (Å)	Magn. coupling[d]	Refs.
$(gua)_2[Cu(ox)_2]$	Elong. Oct	C; S	2.825	3.582	AF	This work
$(apy)_2[Cu(ox)_2]\ 3H_2O$	Elong. Oct	NC; Z	2.701	3.430	AF	This work
			2.814	4.961		
$(py)_2[Cu(ox)_2]\cdot H_2O$	Elong. Oct	C; S	2.890	3.697	AF	[19]
$(pam)_2[Cu(ox)_2]$	Elong. Oct	NC; S	2.883	4.92	AF	[20]
$[Cu_2(ox)_2(H_2oxado)_2(H_2O)_2]$	Elong. Oct	C; Z	2.803	3.751	AF	[27]
$Na_2[Cu(ox)_2]\cdot 2H_2O$	Elong. Oct	C; S	2.803	3.576	AF	[29]
$Cu_2(dpyam)_4(\mu\text{-}ox)](ClO_4)_2\cdot 3H_2O$	Com. Oct	–	–	5.752	F	[39]
$Cu_2(dpyam)_4(\mu\text{-}ox)](BF_4)_2\cdot 3H_2O$	Com. Oct	–	–	5.745	F	[39]
$(H_2CBpy)[Cu(ox)_2]\cdot 2H_2O$	4+1	C; Z	2.798	3.981	F	[41]

[a] gua^+ = guanidinium cation; apy^+ = 2-aminopyridinium cation; py^+ = pyridinium cation; pam^{2+} = propylenediammonium cation; ox = oxalate(2-); H_2ox = oxalic acid; H_2oxado = oxamide dioxime; dpyam = di-2-pyridylamine.
[b] Elong. Oct = elongated octahedron; Com. Oct = compressed octahedron.
[c] C = stacking through coordinated oxygen atom of oxalate; NC = stacking through non-coordinated oxygen atom of oxalate; S = straight chain alignment of copper(II) centers; Z = zigzag chain alignment of copper(II) centers.
[d] AF = antiferromagnetic interactions; F = ferromagnetic interactions.

interaction according to Kahn's model on the in-plane exchange pathway [42].

4. Conclusion

We have synthesized and characterized two novel organic–inorganic hybrid salts, bis(guanidinium) bis(oxalato)cuprate(II), $(CN_3H_6)_2[Cu(C_2O_4)_2]$ (**1**), and bis(2-aminopyridinium) bis(oxalato)-cuprate(II) trihydrate, $(C_5H_7N_2)_2[Cu(C_2O_4)_2]\cdot 3H_2O$ (**2**). In these structures, the $[Cu(C_2O_4)_2]^{2-}$ units are stacked, therefore generating one-dimensional chains with straight (**1**) and zigzag (**2**) alignments of Cu(II) centers. Whereas compound **1** is thermally stable up to ca. 250 °C, compound **2**, by contrast, has a pronounced tendency to release its lattice water molecules at *ca.* 70 °C. Low temperature magnetic study of compounds **1** and **2** reveals weak antiferromagnetic coupling for both. It is worth noting finally, that the present report in all likelihood, lends good grounds to anticipate that a lot is still to be done and understood in this class of hybrid materials, given the wide range of cations that are susceptible to cancel the negative charge of the infinite bis(oxalato)cuprate(II) chains. Therefore, one may expect this assessment to be extendable, not only to homologous organic cations, but to small inorganic charged species such as hydronium (H_3O^+) cations as well. Materials of this type, no doubt, could be well-adapted models in the exploration of the concept of one-dimensional proton conducting solid (1D-PCS) [43–46].

Acknowledgments

The authors are indebted to Prof. Dr. Michel M. Bélombé for the fruitful discussion. J.N. thanks the Deutsche Forschunsgemeinschaft (DFG) for financial support of his three weeks sabbatical at the Institute of Inorganic Chemistry, RWTH Aachen University (Germany), during which this paper was finalized.

Appendix A. Supplementary data

CCDC 982249 and 982250 contains the supplementary crystallographic data for $(CN_3H_6)_2[Cu(C_2O_4)_2]$ (**1**) and $(C_5H_7N_2)_2[Cu(C_2O_4)_2]\cdot 3H_2O$ (**2**). These data can be obtained free of charge via http://www.ccdc.cam.ac.uk/conts/retrieving.html, or from the Cambridge Crystallographic Data Centre, 12 Union Road, Cambridge CB2 1EZ, UK; fax: (+44) 1223 336 033; or e-mail: deposit@ccdc.cam.ac.uk. Supplementary data associated with this article can be found, in the online version, at http://dx.doi.org/10.1016/j.poly.2015.06.023.

References

[1] I. Matulková, J. Cihelka, M. Pojarová, K. Fejfarová, M. Dušek, P. Vaněk, J. Kroupa, R. Krupková, J. Fábry, I. Němec, CrystEngComm 14 (2012) 4625.
[2] O.R. Evans, W.B. Lin, Chem. Mater. 13 (2001) 2705.
[3] X.M. Zhang, M.L. Tong, X.M. Chen, Angew. Chem., Int. Ed. 41 (2002) 1029.
[4] F.R. Gamble, F.J. DiSalvo, R.A. Klemm, T.H. Geballe, Science 168 (1970) 568.
[5] D.B. Mitzi, S. Wang, C.A. Field, C.A. Chess, A.M. Guloy, Science 267 (1995) 1473.
[6] E. Coronado, P. Day, Chem. Rev. 104 (2004) 5419.
[7] P.G. Lacroix, I. Malfant, Chem. Mater. 13 (2001) 441.
[8] M. Clemente-Leon, E. Coronado, C. Marti-Gastaldo, F.M. Romero, Chem. Soc. Rev. 40 (2011) 473.
[9] I. Matulková, J. Cihelka, K. Fejfarová, M. Dušek, M. Pojarová, P. Vaněk, J. Kroupa, M. Šála, R. Krupková, I. Němec, CrystEngComm 13 (2011) 4131.
[10] M. Clemente-Leon, E. Coronado, J.R. Galan-Mascaros, E. Canadell, Inorg. Chem. 39 (2000) 5394.
[11] E. Coronado, J. Galan-Mascaros, C.J. Gomez-Garcia, V. Laukhin, Nature 408 (2000) 447.
[12] O.M. Yaghi, M. O'Keeffe, N.W. Ockwig, H.K. Chae, M. Eddaoudi, T. Kim, Nature 423 (2003) 705.
[13] W. Rekik, H. Naıli, T. Mhiri, T. Bataille, Mater. Res. Bull. 43 (2008) 2709.
[14] E. Pardo, C. Train, H. Liu, L.M. Chamoreau, B. Dkhil, K. Boubekeur, F. Lloret, K. Nakatani, H. Tokoro, S.I. Ohkoshi, M. Verdaguer, Angew. Chem., Int. Ed. 51 (2012) 8356.
[15] B. Das, D.C. Crans, J.B. Baruah, Inorg. Chim. Acta 408 (2013) 204.
[16] D.B. Mitzi, Chem. Mater. 8 (1996) 791.
[17] G.A. Mousdis, G.C. Papavassiliou, C.P. Raptopoulou, A. Terzis, J. Mater. Chem. 10 (2000) 515.
[18] E. Pardo, C. Train, K. Boubekeur, G. Gontard, J. Cano, F. Lloret, K. Nakatani, M. Verdaguer, Inorg. Chem. 51 (2012) 11582.
[19] U. Geiser, B.L. Ramakrishna, R.D. Willett, F.B. Hulsbergen, J. Reedijk, Inorg. Chem. 26 (1987) 3750.
[20] D.R. Bloomquist, J.J. Jansen, C.P. Landee, R.D. Willet, R. Buder, Inorg. Chem. 20 (1981) 3308.
[21] S. Kirschner, Inorg. Synth. 6 (1960) 1.
[22] A. Earnshaw, Introduction to Magnetochemistry, Academic Press, London, 1968.
[23] G.M. Sheldrick, SADABS, University of Göttingen, Göttingen (Germany), 2010.
[24] G.M. Sheldrick, A Short History of SHELX, Acta Crystallogr. Sect. A 64 (2008) 112.
[25] L.J. Farrugia, J. Appl. Crystallogr. 30 (1997) 565.
[26] L.J. Farrugia, J. Appl. Crystallogr. 32 (1999) 837.
[27] J. Nenwa, P.L. Djonwouo, E.N. Nfor, M.M. Bélombé, E. Jeanneau, M. Mbarki, B.P.T. Fokwa, Z. Naturforsch. 69b (2014) 321.
[28] D.T. Keene, M.B. Hursthouse, D.J. Price, Acta Crystallogr. E60 (2004) m378.
[29] A. Gleizes, F. Maury, J. Galy, Inorg. Chem. 19 (1980) 2074.
[30] M.A. Viswamitra, J. Chem. Phys. 37 (1962) 1408.
[31] D.Y. Jeter, W.E. Hatfield, Inorg. Chim. Acta 6 (1972) 523.
[32] D.M. Boghaei, M.M. Najafpour, Anal. Sci. 24 (2008) x23.
[33] L. Golic, N. Bulc, Acta Crystallogr. C44 (1988) 2065.
[34] L. Infantes, S. Motherwell, CrystEngComm 4 (2002) 454.
[35] F.A. Mautner, M. Mikuriya, Y. Naka, F.R. Louka, S.S. Massoud, Polyhedron 85 (2015) 110.
[36] J. Carranza, C. Brennan, J. Sletten, B. Vangdal, P. Rillema, F. Lloret, M. Julve, New J. Chem. 27 (2003) 1775.
[37] F. Tuna, G.I. Pascu, J.P. Sutter, M. Andruh, S. Golhen, J. Guillevic, H. Pritzkow, Inorg. Chim. Acta 342 (2003) 131.
[38] S. Hatscher, H. Schilder, H. Lueken, W. Urland, Pure Appl. Chem. 77 (2005) 497.
[39] S. Youngme, G.A. Albada, N. Chaichit, P. Gunnasoot, P. Kongsaeree, I. Mutikainen, O. Roubeau, J. Reedijk, U. Turpeinen, Inorg. Chim. Acta 353 (2003) 119.

[40] J. Cano, P. Alemany, S. Alvarez, M. Verdaguer, E. Ruiz, Chem. Eur. J. 4 (1998) 476.
[41] W. Li, H.P. Jia, Z.F. Ju, J. Zhang, Inorg. Chem. Commun. 11 (2008) 591.
[42] O. Kahn, Molecular Magnetism, VCH, Weinheim, 1993.
[43] M.M. Bélombé, J. Nenwa, Y.A. Mbiangué, Gouet Bebga, F. Majoumo-Mbé, E. Hey-Hawkins, P. Lönnecke, Inorg. Chim. Acta 362 (2009) 1.
[44] M.M. Bélombé, J. Nenwa, Y.A. Mbiangué, F. Majoumo-Mbé, P. Lönnecke, E. Hey-Hawkins, Dalton Trans. (2009) 4519.
[45] G. Xu, K. Otsubo, T. Yamada, S. Sakaida, H. Kitagawa, J. Am. Chem. Soc. 135 (2013) 7438.
[46] S.S. Nagarkar, S.M. Unni, A. Sharma, S. Kurungot, S.K. Ghosh, Angew. Chem., Int. Ed. 53 (2014) 2638.